Quantification of Vulnerability of Coronary Artery Plaques with MRI and Biomechanics: An Ex vivo Study

J. Zheng[1], D. Tang[2], F. E. Rowold[3], T. Pilgram[4], J. E. Saffitz[5], P. K. Woodard[1]

[1]Radiology, Washington University School of Medicine, St. Louis, MO, United States, [2]Mathematical Sciences, Worcester Polytechnic Institute, Worcester, MA, United States, [3]Biology, Washington University, St. Louis, MO, United States, [4]Radiology, Washington University School of Medicine, ST. Louis, MO, United States, [5]Pathology, Washington University School of Medicine, St. Louis, MO, United States

Introduction

The risk of atherosclerotic plaque disruption is thought to be closely related to not only plaque composition but also rupture triggers such as external mechanical and hemodynamic forces. Magnetic resonance imaging (MRI) has shown great potential for imaging and characterizing atherosclerotic plaque in terms of size, shape, and tissue components. *Our hypothesis is that comprehensive characterization of plaque geometry, components, and critical stress/strain distribution would enhance our ability to identify vulnerable atherosclerotic plaque.* Therefore, the aims of this study were: (1) to develop bioengineering techniques to assess stress/strain distribution within plaques based on MR images of coronary artery plaque specimens; and (2) to quantitatively evaluate the relationships among plaque vulnerability and MR/biomechanical characteristics.

Materials and Methods

Specimens 11 coronary artery segments were selectively collected from 5 autopsy patients (4M, aged 60±15 years). Two patients died of coronary artery disease (CAD). All specimens were fixed in a 10% buffered formalin solution, placed in a polyethylene tube and stored at 4°C within 12 hr after removal from the heart. MRI imaging was performed within 24 hours at room temperature.

MRI Study MR imaging was performed on a 3T Siemens clinical Allegra system. A single transmission/receiver coil with a diameter of 3 cm was used. Images at various TE lengths (T_1- and T_2-weighted contrasts) were obtained of the vessel in cross section. TEs ranged from 20 ms to 70 ms at intervals of 10 ms. Other parameters for each TE image included: TR = 1000 ms, signal average number = 4, FOV = 25 x 19 mm^2, matrix = 256 x 192, slice thickness = 1 mm, and imaging time = 7 min.

Histology After completion of the MR study, transverse sections, 10 μm thick at 1 mm intervals, were obtained from each specimen. These paraffin-embedded sections were stained with hematoxylin and eosin (H&E), Masson's trichrome, and elastin van Gieson's (EVG) stains to identify the plaque components: calcification(Cal), lipid rich necrotic core (LRNC), and fibrotic plaques (FP).

Biomechanic Analysis Classification of plaque components was based on pathological findings, and MR T_1- and T_2-weighted contrasts. Mesh was generated automatically for each component chosen. A finite element software package (ADINA) was modified to perform stress/strain analysis on MR images. Internal blood pressure of 90 mmHg and 150 mmHg were assumed in the mechanical calculation. Maximum principal stress, maximum and minimum of 6 stress (S) and strain (E) components (S-xy, S-xx, S-yy, E-xy, E-xx, E-xy) were obtained for analysis.

Data Analysis T_2 maps were created using a linear regression method. Region-of-interest (ROI) was drawn on each plaque component to calculate its signal intensities on T_1- and T_2-weighted images, as well as T_2 value on corresponding T_2 map. The stenosis of the plaque, the ratios of area of plaque components to the entire plaque area, and contrast-to-noise ratios (LCNR-FP and Cal-FP) were obtained. Based on pathological findings, the vulnerability of each plaque was assigned a score: 0: very stable; 1: stable; 2: slightly unstable; 3: unstable; 4: very unstable. An one-way ANOVA analysis was performed to correlate vulnerability scores and MR/biomechanical features.

Results

The pathological examination revealed that all plaque components were primarily fibrocalcified and necrotic plaques. Intimal thickening was seen in all specimens. Average stenosis was 79 ± 11% in area reduction. No correlation was found between vulnerability scores and contrast-to-noise ratios, or T2 values of LCNR and FT, or stenosis. However, association or consistent trends existed for LCNR area ratio and a certain of stress and strain components (S-xy, and E-xy), particularly at a internal blood pressure of 150 mmHg ($p < 0.05$). Given the small sample size (n=11), these trends were strong. Figure shows MR images and stress maps from two patients with CAD and without CAD. While the CAD patient shows slightly smaller stenosis (83%) than the non-CAD patient (91%), the plaque in the CAD patient was determined to be stable. In contrast, images in the non-CAD patient reveals a large LCNR and calcification and the plaque is pathologically vulnerable (score = 4). The maximum of stress (S-xy) and strain (E-xy) are 90-125% higher than their counterparts in the CAD patient. Furthermore, the compression stress and strain (minimum values) are also 130-230% higher in the plaque of non-CAD patient.

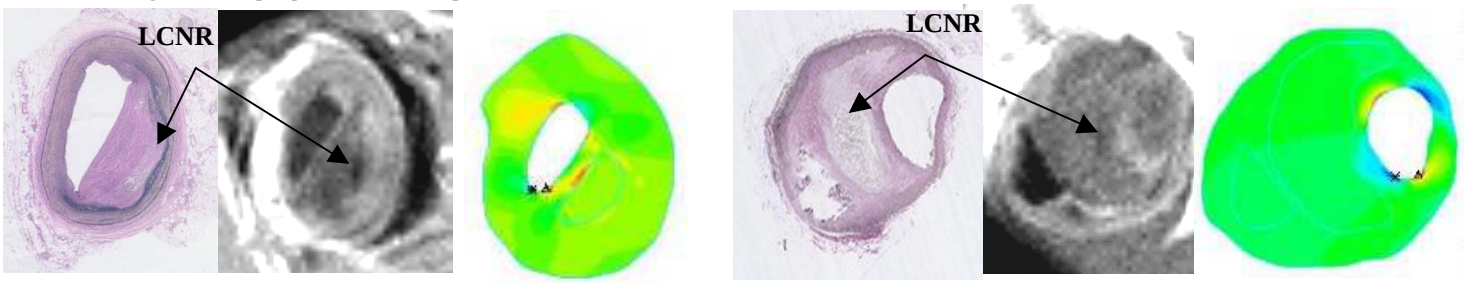

(a) (b)

Figure. Two groups of images showing coronary artery specimens from a (a) CAD patient and (b) non-CAD patient. In each group, from left to right: histogram, T2-weighted MR image, and stress (S-xy) map. Small LCNR was shown in (a), but a large lipid core is shown in (b). The label "Δ" and "∗" indicate locations of maximum and minimum stress, respectively.

Conclusion

This is the first time that high resolution ex vivo MR images have been used to assess comprehensive characteristics of coronary artery atherosclerotic plaques in terms of plaque components, size, and stress/strain distributions. Vulnerable plaques are found to be strongly associated with large lipid pools and certain critical stress/strain conditions. These findings provide an impetus to perform further research on a larger population of samples to define effective quantitative biomarkers to non-invasively assess the vulnerability of atherosclerotic plaque in vivo.

Acknowledgement

This project is supported in part by the Charles E. Culpeper Biomedical Pilot Initiative grant.